

## OPTIMIZED LINEAR COMBINATIONS OF CHANNELS FOR COMPLEX MULTIPLE-COIL $B_1$ FIELD ESTIMATION WITH BLOCH-SIEGERT $B_1$ MAPPING IN MRI

Feng Zhao<sup>1</sup>, Jeffrey A. Fessler<sup>2</sup>, Steven M. Wright<sup>3</sup>, Joseph V. Rispoli<sup>4</sup>, Douglas C. Noll<sup>1</sup>

<sup>1</sup>BME Dept., The University of Michigan, <sup>2</sup>EECS Dept., The University of Michigan

<sup>3</sup>ECE Dept., Texas A&M University, <sup>4</sup>BME Dept., Texas A&M University

**Abstract**—Bloch-Siebert  $B_1$  mapping for multiple-channel parallel excitation systems usually produces noisy estimates in low intensity regions. Methods that use linear combinations of multiple coils have been proposed to mitigate this problem. However, little work has been done to optimize these coil combinations to improve the signal-to-noise ratio of  $B_1$  mapping in a robust way. In this paper, we propose a Cramer-Rao Lower Bound analysis based method to optimize the coil combination matrix by minimizing the variance of  $B_1$  map estimation for the previously proposed Bloch-Siebert  $B_1$  mapping method. We illustrate how optimizing the coil combinations yields improved  $B_1$  estimates in a simulation of brain imaging with a 3T MRI scan.

**Index Terms**—Magnetic resonance imaging,  $B_1$  mapping, Bloch-Siebert  $B_1$  mapping, Cramer-Rao Lower Bound

### I. INTRODUCTION

In MRI with parallel excitation (PEX), it is critical to rapidly and accurately estimate the magnitude and relative phase of each coil's  $B_1^+$  field. Numerous methods have been proposed to map  $B_1$  magnitude, such as actual flip angle imaging (AFI) [1] and Bloch-Siebert (BS)  $B_1$  mapping [2]. For PEX pulse design, relative  $B_1$  phase, i.e., the phase of one coil relative to that of all the other coils, is needed and is typically mapped by successively exciting the same object with each coil and receiving the signal by a common coil.

Recently, BS  $B_1$  mapping has become popular because it is fast and relatively accurate over a wide dynamic range [2]. However, a disadvantage of this phase-based method is that estimation in low magnitude regions may suffer from low signal-to-noise ratio (SNR), due to insufficient excitation or low spin densities. Furthermore, it is time-consuming and information redundant to estimate  $B_1$  phase by a second set of scans. To mitigate this problem, we recently developed a regularized BS  $B_1$  mapping method to estimate the complex multi-coil  $B_1$  field with no additional scans needed for phase estimation [3].

To improve SNR, linear combinations of PEX channels are used to narrow the dynamic range of effective  $B_1$  field in [3], where typically “all-but-one” strategies [4-5] are applied. However, these strategies are likely to be suboptimal in practice, as the power of different channels for the object could be uneven, the relative phase between channels could be far from what is assumed. Optimization of linear coil combinations has been discussed in [6]; however, only a single complex parameter in the combination matrix was optimized over a limited range in an empirical way, and the method evaluated results according to two criteria, i.e., the dynamic range of the composite  $B_1$  maps and the condition number of the combination matrix, which sometimes are hard to balance.

In this paper, we propose a method to optimize linear coil combinations in [3] based on Cramer-Rao Lower Bound (CRLB) analysis. The proposed method is able to optimize over all the

elements of the combination matrix, which provides the most flexibility. Evaluation of the combinations is directly based on the variance of the complex  $B_1$  field estimates without the need to balance multiple criteria. Simulated Annealing is used to optimize this highly nonlinear problem. The proposed method is demonstrated by a simulation study where several practical considerations are discussed.

### II. REGULARIZED ESTIMATION OF THE COMPLEX MULTICHANNEL $B_1$ FIELD WITH BS $B_1$ MAPPING

#### A. Linear Combinations of Coils in $B_1$ Mapping

To improve SNR, our method [3] estimates multi-channel  $B_1$  field by acquiring standard BS  $B_1$  mapping data with multiple coils turned on at each time. As shown in (1), the composite complex  $B_1$  field, i.e.,  $\tilde{C}_n(\mathbf{r})$ , is the linear combination of the individual complex  $B_1$  maps, i.e.,  $C_m(\mathbf{r})$ :

$$\tilde{C}_n(\mathbf{r}) = \sum_{m=1}^N \alpha_{n,m} C_m(\mathbf{r}) \quad (1)$$

where  $n = 1, 2, \dots, N$ ,  $N$  is the number of channels,  $\mathbf{r}$  denotes the spatial locations, and  $\alpha_{n,m}$  is the user-defined complex scalar weighting for the  $m$ th individual coil in the  $n$ th scan. The goal is to optimize over  $\alpha_{n,m}$  to obtain the highest SNR. Both the composite complex  $B_1$  maps and the individual complex  $B_1$  maps can be expressed as magnitude and phase parts:

$$\tilde{C}_n(\mathbf{r}) = \tilde{B}_n(\mathbf{r}) e^{i\tilde{\phi}_n(\mathbf{r})}, \quad C_m(\mathbf{r}) = B_m(\mathbf{r}) e^{i\phi_m(\mathbf{r})} \quad (2)$$

#### B. The Signal Model

The standard BS  $B_1$  mapping works by applying an off-resonance RF pulse, which is called Bloch-Siebert (BS) pulse, after the regular excitation pulse [2]. This method typically needs 2 scans to measure the  $B_1$  magnitude of each coil, thus 2N scans are required for an N-channel PEX system.

Using the same coil combinations for the BS pulse and the corresponding excitation pulse, we are able to estimate both  $B_1$  magnitude and (relative) phase with only 2N scans [3]. The signal models for the noiseless BS data (reconstructed images) of the  $n$ th pair of scans, i.e.,  $\tilde{S}_n^+(\mathbf{r})$  and  $\tilde{S}_n^-(\mathbf{r})$ , are:

$$\begin{cases} \tilde{S}_n^+(\mathbf{r}) = M_n^+(\mathbf{r}) e^{i[K_{BS}^+(\mathbf{r})\tilde{B}_n(\mathbf{r})^2 + \tilde{\phi}_n^+(\mathbf{r})]} \\ \tilde{S}_n^-(\mathbf{r}) = M_n^-(\mathbf{r}) e^{i[K_{BS}^-(\mathbf{r})\tilde{B}_n(\mathbf{r})^2 + \tilde{\phi}_n^-(\mathbf{r})]} \end{cases} \quad (3)$$

where  $n = 1, 2, \dots, N$ ; the superscripts  $\pm$  denote the scan that has the BS pulse with  $+\omega_{RF}$  or  $-\omega_{RF}$  off-resonance frequency;  $M_n^\pm(\mathbf{r}) \triangleq \sin(\mu\tilde{B}_n(\mathbf{r}))m_n^\pm(\mathbf{r})$ ,  $\mu$  is the ratio between the flip angle and  $\tilde{B}_n(\mathbf{r})$ ,  $m_n^\pm(\mathbf{r})$  is the magnitude related to spin density,  $T_1$ ,  $T_2$ ,  $T_R$ ,  $T_E$ , flip angle, receive sensitivity, magnetization transfer (MT) effect, etc.;  $\tilde{\phi}_n^+(\mathbf{r}) \triangleq \tilde{\phi}_n^+(\mathbf{r}) + \phi_b(\mathbf{r})$ , and  $\phi_b(\mathbf{r})$  is the corresponding background phase;  $K_{BS}^\pm(\mathbf{r})$  is the BS pulse constant that

incorporates the  $B_0$  field map [2]. The unknown variables are  $\tilde{B}_n(\mathbf{r})$  and  $\tilde{\phi}_n(\mathbf{r})$ . Moreover, we modeled additive identical independent (i.i.d.) complex Gaussian noise, i.e.,  $\epsilon_n^\pm(\mathbf{r})$ , to the signal:

$$\begin{cases} S_n^+(\mathbf{r}) = \tilde{S}_n^+(\mathbf{r}) + \epsilon_n^+(\mathbf{r}) \\ S_n^-(\mathbf{r}) = \tilde{S}_n^-(\mathbf{r}) + \epsilon_n^-(\mathbf{r}) \end{cases} \quad (4)$$

where  $S_n^\pm(\mathbf{r})$  are the noisy signals from the  $n$ th pair of scans.

### C. Regularized Estimation of $B_1$ Magnitude and Phase [3]

Assuming that the composite  $B_1$  magnitude,  $\tilde{B}_n(\mathbf{r})$ , and the relative phase, e.g.,  $\tilde{\phi}_n(\mathbf{r}) - \tilde{\phi}_1(\mathbf{r})$  are spatially smooth, we apply finite differencing matrix  $C$  to penalize roughness of the maps. The regularizer proposed in [7] is used to prevent phase wraps of  $\tilde{\phi}_n(\mathbf{r}) - \tilde{\phi}_1(\mathbf{r})$ . With maps discretized into vectors (bolded), the final regularized maximum-likelihood cost function is:

$$\begin{aligned} \Psi(\tilde{\mathbf{B}}, \tilde{\boldsymbol{\phi}}, \mathbf{M}) = & \sum_{n=1}^N \sum_{\delta=\pm, -} \left\| S_n^\delta - \mathbf{M}_n^\delta e^{i[K_{BS}^\delta \tilde{B}_n^2 + \tilde{\phi}_n']} \right\|^2 \\ & + \beta_1 \sum_{n=1}^N \|C \tilde{\mathbf{B}}_n\|^2 + \beta_2 \sum_{n=2}^N \left\| C e^{i[\tilde{\phi}_n' - \tilde{\phi}_1']} \right\|^2 \end{aligned} \quad (5)$$

where  $\beta_1$  and  $\beta_2$  are the scalar regularization parameters,  $\mathbf{M} = [\mathbf{M}_1^{+T}, \dots, \mathbf{M}_N^{+T}, \mathbf{M}_1^{-T}, \dots, \mathbf{M}_N^{-T}]^T$ ,  $\tilde{\mathbf{B}} = [\tilde{\mathbf{B}}_1^T, \dots, \tilde{\mathbf{B}}_N^T]^T$ , and  $\tilde{\boldsymbol{\phi}} = [\tilde{\phi}_1', \dots, \tilde{\phi}_N']^T$ . The cost function is iteratively minimized by cyclically updating  $\tilde{\mathbf{B}}$ ,  $\tilde{\boldsymbol{\phi}}$  and  $\mathbf{M}$ . Once  $\tilde{\mathbf{B}}$  and  $\tilde{\boldsymbol{\phi}}$  are estimated, the magnitude and relative phase of the original coils can be derived according to (6), where  $\phi_n'(\mathbf{r}) = \phi_n(\mathbf{r}) + \phi_b(\mathbf{r})$  which does not change the relative phase of the  $n$ th coil.

$$\begin{bmatrix} B_1(\mathbf{r}) e^{i\phi_1'(\mathbf{r})} \\ \vdots \\ B_N(\mathbf{r}) e^{i\phi_N'(\mathbf{r})} \end{bmatrix} = A^{-1} \begin{bmatrix} \tilde{B}_1(\mathbf{r}) e^{i\tilde{\phi}_1(\mathbf{r})} \\ \vdots \\ \tilde{B}_N(\mathbf{r}) e^{i\tilde{\phi}_N(\mathbf{r})} \end{bmatrix} \quad (6)$$

$$\text{where } A \triangleq \begin{bmatrix} \alpha_{1,1} & \cdots & \alpha_{1,N} \\ \vdots & \ddots & \vdots \\ \alpha_{N,1} & \cdots & \alpha_{N,N} \end{bmatrix}.$$

## III. OPTIMIZATION OF THE COIL COMBINATIONS

The basic idea of the proposed method is to derive a formula for the variance of the complex  $B_1$  field estimates in terms of the combination matrix  $A$  by using CRLB analysis, which is the foundation for optimizing over  $A$ .

### A. The Signal Model with Approximations

To simplify the noise analysis, we make some reasonable approximations for the signal model equations (4): asymmetric MT effect [2] is ignored so that  $M_n^+(\mathbf{r}) \approx M_n^-(\mathbf{r}) \triangleq M_n(\mathbf{r})$ , and the off-resonance effects in  $K_{BS}^\pm(\mathbf{r})$  are ignored so that  $K_{BS}^+(\mathbf{r}) \approx -K_{BS}^-(\mathbf{r}) \triangleq K$  which is a constant. We assume the real and imaginary parts of the i.i.d. Gaussian noise are uncorrelated and distributed as  $N(0, \sigma^2)$  where  $\sigma^2$  is the variance, so the signals of each pixel are distributed as in (7):

$$\begin{cases} S_r^+ \sim N(M \cos(KB^2 + \phi), \sigma^2) \\ S_i^+ \sim N(M \sin(KB^2 + \phi), \sigma^2) \\ S_r^- \sim N(M \cos(-KB^2 + \phi), \sigma^2) \\ S_i^- \sim N(M \sin(-KB^2 + \phi), \sigma^2) \end{cases} \quad (7)$$

where subscripts  $n$ , indices  $\mathbf{r}$ , primes and tildes are omitted for simplicity, and subscripts  $r/i$  denote the real/imaginary parts.

### B. Cramer-Rao Lower Bound Analysis

The CRLB is a lower bound on the covariance of any unbiased estimator under certain regularity conditions. The CRLB can be achieved by unbiased maximum likelihood estimators (MLE). This work tries to improve the quality of the raw data before applying regularized estimation, so the effective estimators are equivalent to the estimators in (5) with  $\beta_1 = \beta_2 = 0$  which yields MLE.

Vectorizing (7) yields the nonlinear model:

$$\mathbf{y} = \boldsymbol{\mu}(\boldsymbol{\theta}) + \boldsymbol{\epsilon} \quad \text{with } \boldsymbol{\epsilon} \sim N(\mathbf{0}, \sigma^2 \mathbf{I}) \quad (8)$$

where  $\mathbf{y} = [S_r^+, S_i^+, S_r^-, S_i^-]^T$ ,  $\boldsymbol{\mu}(\boldsymbol{\theta}) = [M \cos(KB^2 + \phi), M \sin(KB^2 + \phi), M \cos(-KB^2 + \phi), M \sin(-KB^2 + \phi)]^T$ ,  $\boldsymbol{\theta} = [B, \phi]^T$ . The regularity condition is satisfied, i.e., the expectation of the gradient of log-likelihood  $L(\boldsymbol{\theta})$  is zero. Then the Fisher information  $F(\boldsymbol{\theta})$  can be derived as follows:

$$F(\boldsymbol{\theta}) \triangleq E \left[ (\nabla L(\boldsymbol{\theta})) (\nabla L(\boldsymbol{\theta}))^H \right] = \frac{2M^2}{\sigma^2} \begin{bmatrix} 4K^2 B^2 & 0 \\ 0 & 1 \end{bmatrix} \quad (9)$$

According to CRLB, we have the following:

$$\text{cov}([\tilde{B}, \tilde{\phi}]) \geq F(\boldsymbol{\theta})^{-1} \quad (10)$$

By using Taylor expansion approximation, we have:

$$\text{var} \left( \tilde{B}_{n,r}(A) e^{i\tilde{\phi}_{n,r}(A)} \right) \geq \frac{\sigma^2}{2M_{n,r}^2(A)} \left[ \tilde{B}_{n,r}^2(A) + \frac{1}{4K^2 \tilde{B}_{n,r}^2(A)} \right] \quad (11)$$

where we have inserted subscripts  $n$ , indices  $\mathbf{r}$ , primes and tildes except that we put  $\mathbf{r}$  to the subscripts and make  $A$  be the argument, as  $A$  is the variable of this optimization problem. Assuming noise is independent between scans, we derived the variances of the complex  $B_1$  estimates at  $\mathbf{r}$ :

$$\text{var}(\hat{C}_{n,r}(A)) \triangleq \text{var} \left( \tilde{B}_{n,r}(A) e^{i\tilde{\phi}_{n,r}(A)} \right) \geq V_{n,r}(A) \quad (12)$$

with  $V_{\mathbf{r}}(A) \triangleq [V_{1,r}(A), \dots, V_{N,r}(A)]^T$

$$\triangleq \text{diag} \left\{ A^{-1} \text{diag} \left\{ \frac{\sigma^2}{2M_{n,r}^2(A)} \left[ \tilde{B}_{n,r}^2(A) + \frac{1}{4K^2 \tilde{B}_{n,r}^2(A)} \right] \right\} A^{-H} \right\}$$

where  $n = 1, \dots, N$ , and  $\text{diag}\{\mathbf{z}\}$  denotes either the diagonal matrix with the vector  $\mathbf{z}$  the diagonal entries or the vector that contains the diagonal entries of the matrix  $\mathbf{z}$ .

### C. Optimize Linear Combinations of Array Elements

We propose to optimize  $B_1$  estimation by minimizing the lower bound of noise-to-signal ratio (NSR), which is defined to be the ratio between  $\sqrt{V_{n,r}(A)}$  and  $B_n(\mathbf{r})$  as shown in (13). Moreover, to define a scalar that evaluates the noise performance of the whole 2D or 3D  $B_1$  field of the  $N$  coils, we minimize the maximal NSR over all the spatial locations and channels. A practical consideration is that PEX systems have power limits, so the maximal magnitude of the elements of  $A$  is bounded according to the hardware limits. Therefore, the final expression of this optimization problem is:

$$\hat{A} = \underset{A \in \mathbb{C}^{N \times N}}{\text{argmin}} \{P(A)\} \quad (13)$$

$$\text{with } P(A) \triangleq \begin{cases} \max_{n,r} \frac{\sqrt{V_{n,r}(A)}}{B_n(\mathbf{r})} & \text{if } \max_{m,n} |\alpha_{m,n}| \leq \lambda \\ +\infty & \text{if } \max_{m,n} |\alpha_{m,n}| > \lambda \end{cases}$$

where  $\lambda$  is the power limit of the PEX system.

### D. Optimization Using Simulated Annealing (SA)

The cost function in (13) is highly nonlinear and non-convex in terms of  $A$ , so it is hard to find the global minimum without a time-consuming exhaustive search. In practice, however, we only need to keep the noise level below a certain reasonable level, instead of exhaustively searching for the best choice. Since the size of  $A$  is small, the SA method, which is implemented in Matlab Optimization Toolbox, can find a reasonably good local minimum efficiently.

### E. Other Practical Considerations

To apply (12) and (13), we need to know the true  $B_1$  maps and the image magnitude  $M_{n,r}(A)$  which is a known function of transmit and receive sensitivities, spin densities,  $T_1$  and  $T_2$  maps. We propose to avoid these impractical requirements for in-vivo imaging as follows. Spin densities and  $T_2$  values are set to be the average values of a canonical brain, while  $T_1$  map is uniformly set to be the maximal value.  $B_1^-(\mathbf{r})$  is set to be uniform ( $B_0 \leq 3T$ ) or obtained from an off-line phantom scan ( $B_0 > 3T$ ). An off-line phantom  $B_1$  mapping is used as the “true” transmit  $B_1$  for the optimization, and the  $B_1$  phase can also be obtained by a set of fast on-line low resolution scans.

## IV. SIMULATION STUDY

### A. Simulation Setup

A finite-difference time-domain (FDTD) simulation was done to generate 2D magnetic fields for an eight-channel parallel excitation array for brain imaging in 3T, which is used as the true  $B_1$  maps in the simulations. We used a set of brain tissue parameter

noise to the noiseless images generated based on (3), we simulated the raw data in image domain acquired by SPGR-based BS  $B_1$  mapping sequence. The matrix size of these 2D images is  $64 \times 64$ . Note that we optimize the coil combination matrix  $A$  before simulating the raw data. In the data simulation, the standard deviation of the Gaussian noise stayed the same and the SNR of raw data was around 25 dB depending on the specific coil combinations. In this study, we used the standard non-regularized method to reconstruct the  $B_1$  magnitude and phase.

We used approximated parameters for the optimization step.  $T_2$  maps and spin densities were set to be the average value of a canonical brain tissue;  $T_1$  maps were set to be the maximal value of brain tissue. Since the true receive coil is single-channel in 3T which is relatively uniform, we used a uniform  $B_1^-$  map for the optimization. Furthermore, we did another FDTD simulation for a uniform phantom with the same coil configurations as the simulation for a brain, and the space occupied by the phantom covered the brain used in the previous simulation so that the phantom  $B_1$  maps can be cropped to the brain size for the optimization. For the  $B_1$  phase specifically, other than using the

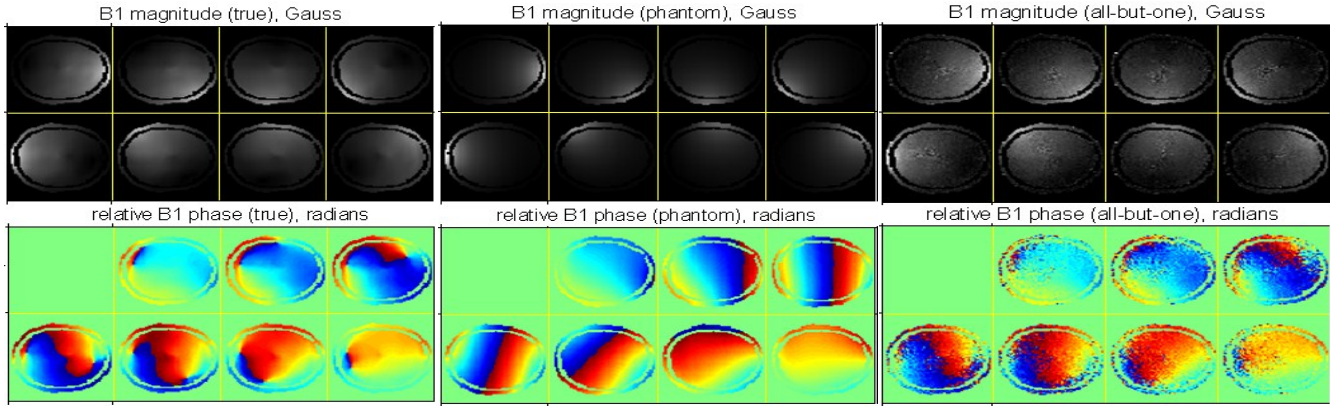


Fig. 1: the true  $B_1$  maps

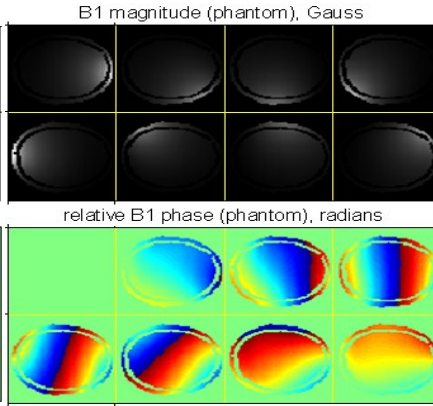


Fig. 2: the offline phantom  $B_1$  maps

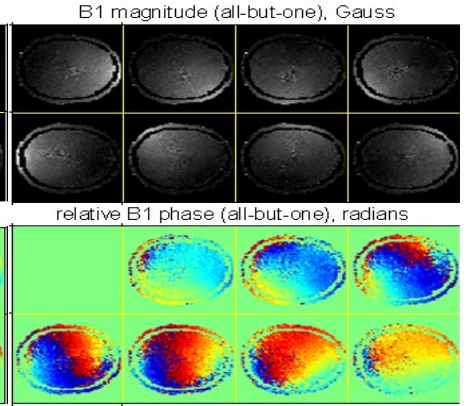


Fig. 3: estimates by all-but-one method

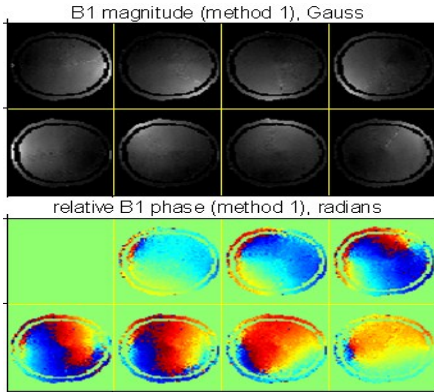


Fig. 4: estimates by method 1

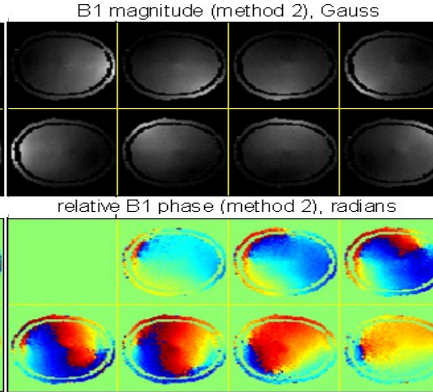


Fig. 5: estimates by method 2

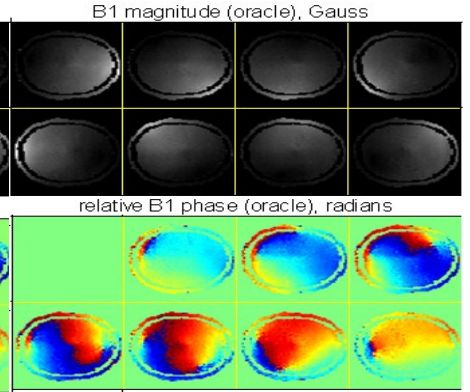


Fig. 6: the oracle results

maps, e.g.,  $T_1$  maps,  $T_2$  maps and spin densities, from BrainWeb database [8] as the true values for generating images produced by the BS sequence. The image magnitude is generated based on the signal equation of spoiled GRE (SPGR) sequence [9] with image parameters:  $T_R = 200 \text{ ms}$ ,  $T_E = 10 \text{ ms}$ . The BS induced phase is simulated based on BS pulses with  $\pm 4 \text{ kHz}$  off-resonance ( $K_{BS} = 76.9 \text{ rad/G}^2$ ) and a realistic  $B_0$  field map acquired from a brain on a 3T GE scanner (ranging from  $-86 \text{ Hz}$  to  $25 \text{ Hz}$ ). Furthermore, the  $B_1^-$  map was acquired from a real single-channel body receive coil of the 3T GE scanner. By adding some i.i.d. complex Gaussian

phantom  $B_1$  phase which will be called “method 1”, we also simulated an on-line low resolution ( $32 \times 32$  matrix) fast scan of brain using one transmit coil at a time to obtain the relative  $B_1$  phase, which will be called “method 2”. Circulant structure was assumed for the matrix  $A$ , and the optimization algorithm was initialized with the all-but-one combination, e.g.,  $\alpha_{1,1} = 0, \alpha_{1,2} = \dots = \alpha_{1,N} = 1$ . The threshold  $\lambda$  in (13) was set such that the RF power does not exceed 0.15 Gauss.

Table I: Statistics of the Results in Fig. 3-6

	all-but-one	method 1	method 2	oracle
NRMSE of $B_n(\mathbf{r})$	18.0%	9.09%	5.92%	5.85%
RMSE of $\phi_n(\mathbf{r})$ , radians	0.645	0.355	0.281	0.245

### B. Results

Fig. 1-2 show the true  $B_1$  magnitude and relative phase on the brain (Fig. 1) and those on the phantom (masked by the brain shape, Fig. 2) which were used for the optimization. The “all-but-one” strategy we used was  $\alpha_{1,1} = 0$ ,  $\alpha_{1,2} = \dots = \alpha_{1,2} = 1$ , which produced very noisy estimates as shown in Fig. 3. The results of the optimized coil combinations are shown in Fig. 4-5, where both method 1 and method 2 improve the estimations significantly but method 2 works better. Lastly, we show the oracle results where the optimization was based on the true transmit  $B_1$  maps, which were only slightly better than those of method 2. Table I summarizes the results of Fig. 3-6 quantitatively. Note that all the magnitude maps are in the grayscale from 0 to 0.07 Gauss, and all the phase maps are in the colorscale from  $-\pi$  to  $\pi$ .

### V. DISCUSSION AND CONCLUSIONS

According to the results of the proposed method, the optimization results are insensitive to inaccurate  $T_2$ , spin densities and receive sensitivities for 3T brain imaging. However, the results are more sensitive to different  $T_1$  values which are not shown; we empirically found that using uniform maps with the maximal  $T_1$  is generally more robust than uniform maps with other  $T_1$  values, e.g., the average  $T_1$ , at least for the case of SPGR sequence. Because the magnitude is  $T_1$ -weighted and long  $T_1$  corresponds to low signal, which means using  $T_1$  smaller than any actual tissue  $T_1$  for the optimization may make estimates of the longer  $T_1$  regions noisy.

As seen in Fig. 1-2,  $B_1$  phase of the phantom is likely to be far from that of the brain, whereas the magnitude parts are relatively close. As expected, method 2 which used more accurate  $B_1$  phase worked better than method 1, and method 2 worked almost as well as the oracle optimization due to insensitivity to small errors of the  $B_1$  magnitude estimates by the phantom. In fact, some failure results of method 1 using some other phantoms are not shown, while method 2 is usually robust. The cost of method 2 is the requirement of an online optimization and a fast pre-scan, which is a reasonable tradeoff for better robustness in practice.

Although for low noise levels, good estimates of  $B_1$  maps may be achieved using the all-but-one combinations with the regularized method in [3], the proposed coil combinations produce raw data with much better SNR, which promotes robustness of the regularized BS  $B_1$  mapping method. Sometimes, the results of the

proposed method could be good enough to use without further regularization, which can somewhat simplify implementation and eliminates the need to choose regularization parameters.

This simulation was done for the SPGR sequence, but the similar principle can be applied for any other typical BS  $B_1$  mapping compatible sequences. A future work is to explore the method for  $B_1$  mapping in other parts of human body. Moreover, we believe that the CRLB based noise analysis used in this work for BS  $B_1$  mapping can be applied to coil combinations of other  $B_1$  mapping methods, e.g., AFI [1].

### ACKNOWLEDGMENT

This work was supported by NIH Grant R01 NS58576.

### REFERENCES

- [1] V. Yarnykh, “Actual flip-angle imaging in the pulsed steady state: A method for rapid three-dimensional mapping of the transmitted radiofrequency field,” *Magnetic resonance in Medicine*, vol. 57, no. 1, pp. 192–200, 2007.
- [2] L. Sacolick, F. Wiesinger, I. Hancu, and M. Vogel, “ $B_1$  mapping by Bloch-Siegert shift,” *Magnetic Resonance in Medicine*, vol. 63, no. 5, pp. 1315–1322, 2010.
- [3] F. Zhao, J.A. Fessler, J-F Nielsen, and D.C. Noll, “Regularized estimation of magnitude and phase of multiple-coil  $B_1$  field via Bloch-Siegert  $B_1$  mapping,” in *Proceedings of the 20th International Society for Magnetic Resonance in Medicine*, 2012.
- [4] K. Nehrke and P. Bornert, “Improved  $B_1$ -mapping for multi RF transmit systems,” in *Proceedings of the 16th Scientific Meeting of International Society for Magnetic Resonance in Medicine*, 2008, p. 353.
- [5] D. Brunner and K. Pruessmann, “ $B_1+$  interferometry for the calibration of RF transmitter arrays,” *Magnetic Resonance in Medicine*, vol. 61, no. 6, pp. 1480–1488, 2009..
- [6] S. Malik, D. Larkman, and J. Hajnal, “Optimal linear combinations of array elements for  $B_1$  mapping,” *Magnetic Resonance in Medicine*, vol. 62, no. 4, pp. 902–909, 2009.
- [7] F. Zhao, D. Noll, J. Nielsen, and J. Fessler, “Separate magnitude and phase regularization via compressed sensing,” *Medical Imaging, IEEE Transactions on*, vol. 31, no. 9, pp. 1713–1723, 2012.
- [8] <http://www.bic.mni.mcgill.ca/brainweb/>
- [9] E. M. Haacke, R. W. Brown, M. R. Thompson, R. Venkatesan, *Magnetic Resonance Imaging: Physical Principles and Sequence Design*, J. Wiley & Sons, 1999